INTERNATIONAL JOURNAL FOR NUMERICAL METHODS IN FLUIDS, VOL. 10, 729–740 (1990)

APPLICATION OF A VORTEX LATTICE NUMERICAL MODEL IN THE CALCULATION OF INVISCID INCOMPRESSIBLE FLOW AROUND DELTA WINGS

G. BANDYOPADHYAY

Aeronautical Engineering Department, Indian Institute of Technology, Kharagpur 721302, India

SUMMARY

The flow over a flat plate delta wing at incidence and in sideslip is studied using vortex lattice models based on streamwise penelling. For the attached flow problem the effect of sideslip is simulated by modifying the standard vortex lattice model for zero sideslip by aligning the trailing vortices aft of the wing along the resultant flow direction. For the separated flow problem a non-linear vortex lattice model is developed for both zero and non-zero sideslip angles in which the shape and position of the leading edge separation vortices are calculated by an iterative procedure starting from an assumed initial shape. The theoretical values are compared with available theoretical and experimental results.

KEY WORDS Delta wing Leading edge separation Free vortex Iteration Sideslip Rolling moment Dihedral

1. INTRODUCTION

The flow over a flat plate delta wing at moderate-to-high angle of attack has been studied extensively. Early attempts[1–4] were based on the assumption of slender wing theory. Fully three-dimensional techniques based on the vortex lattice concept were later developed.[5–7] In addition to the standard vortex lattice, these methods use a number of non-intersecting vortex lines to represent the wake generated by the leading edge, tip and trailing edge separation. An iterative procedure is used to determine the position of these lines from assumed initial values. A fairly comprehensive method has been developed[8, 9] by the Boeing Aircraft Company. The method is based on a higher-order formulation in which the wing, the rolled-up vortex sheet and the wake are represented by quadratic doublet and linear source distributions. The strength of the singularity distribution as well as the shape and position of the vortex sheet are computed iteratively.

The vortex lattice method is one of the currently used numerical methods for potential flow calculation. However, a variety of other methods have been developed to study the flow over a flat plate delta wing, e.g. the multi-vortex model,[10] the leading edge suction analogy,[11] the slender body panel method,[12] the hybrid method[13] and the vortex particle method.[14] A review of the various methods is presented in Reference 15.

For a sideslipping flat plate delta wing, Pullin[16] and Jones[17] have developed methods within the framework of the slender wing assumption. Pullin's method[16] is based on an integro-differential equation formulation due to Legendre.[1] The model developed by Jones[17] can be considered to be an extension of Smith's theory[4] when the wing is in sideslip. The method uses a different conformal transformation suitable for the asymmetric case.

0271–2091/90/070729–12$06.00

Received December 1988
Revised June 1989

The availability of numerical methods for the asymmetric case is not so common and there is a need to assess how far the numerical models developed for the symmetric case can be extended to the asymmetric case. Katz[18] developed a method for a delta wing in sideslip using an unsteady vortex lattice model. Starting with a solution at time $t = 0$, the vortex sheets emanating from the leading edge and subsequent roll-up are calculated by releasing vortex segments at each time interval Δt. Results have also been obtained with this model for a wing in constant roll and a wing displaying coning motion.

The various vortex lattice models developed for calculating attached and separated flow about delta wings use a variety of discretization schemes (Figure 1). Rectangular panelling is used by Kandil *et al.*[7] and Katz,[18] while in the hybrid method of Jepps[13] conical panelling is used. Streamwise panelling is used by Javed and Hancock[19] for a variety of wing configurations in attached flow.

Among the different discretization schemes, conical panelling is restricted to delta planforms, whereas rectangular panelling is more flexible and is used by Kandil *et al.*[7] for rectangular, delta and untapered swept configurations. Perhaps the most versatile discretization scheme uses streamwise panelling (Figure 1). The main advantage of such panelling is the easy representation of arbitrary planform shapes.

In this paper, attached and separated flow models based on the vortex lattice concept using streamwise panelling have been developed to study the flow over flat plate delta wings at incidence and in sideslip.

2. DESCRIPTION OF FLOW MODEL

2.1. Attached flow model

When the flow is attached, a planar vortex lattice model is used. In this model the wing chordal surface plane $Z = 0$ is divided into M chordwise and N spanwise panels as shown in Figure 2. Each panel is represented by a horseshoe vortex of constant strength, which varies from panel to panel. This model with sideslip involves a modification so that the trailing vortices in each panel aft of the trailing edge are taken along the resultant flow direction rather than along the chordal direction. The collocation points are taken to be the three-quarters-panel chordwise position for both symmetric and sideslip cases.

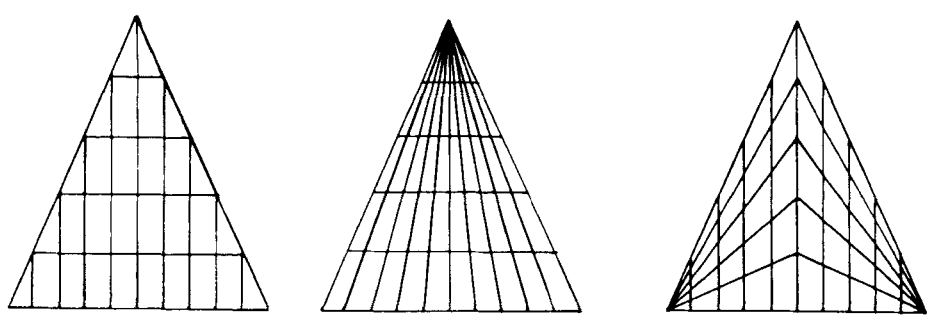

Figure 1. Various discretized models

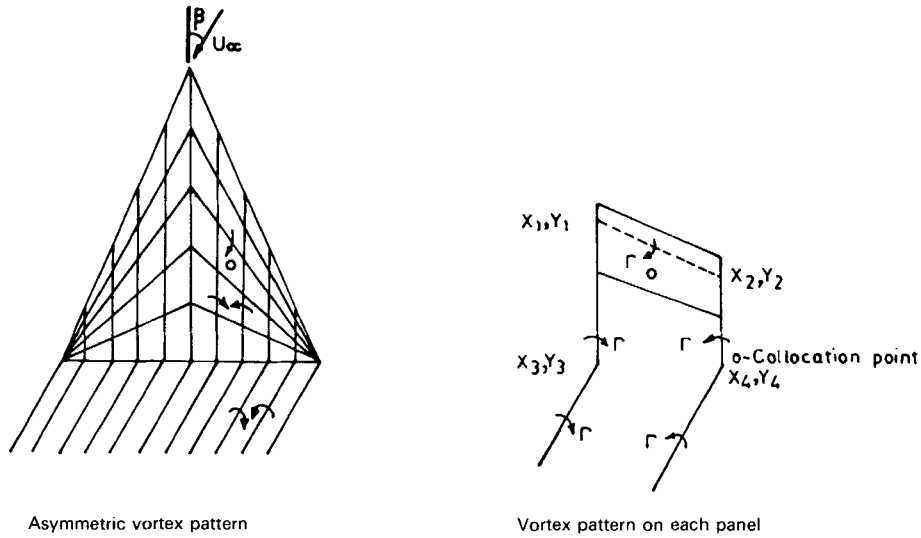

Figure 2. Attached flow model for wing in sideslip

The problem is to determine the strengths of the horseshoe vortices, $\Delta\Gamma_i$, $i = 1, M \times N$. This is done by satisfying the boundary condition of zero normal flow at all collocation points, which results in a system of simultaneous linear algebraic equations.

In general matrix form,

$$[A_{ji}]\{\Delta\Gamma_i\} = \{W_j\}, \tag{1}$$

where

$$W_j = \begin{cases} -U_\infty\alpha + U_\infty\beta\Gamma & \text{for the port wing,} \\ -U_\infty\alpha - U_\infty\beta\Gamma & \text{for the starboard wing,} \end{cases} \tag{2}$$

A_{ji} is the influence coefficient matrix, U_∞ is the onset flow speed, β is the angle of sideslip and Γ is the wing dihedral.

In the asymmetric case, both the 'bound' and 'trailing' vortices on the wing sustain lift force since there is a component of free stream resultant velocity normal to both. There is no lift on the trailing vortices aft of the wing because they are in the direction of the resultant free stream.

Once the system of linear algebraic equations, equation (1), has been solved to give the unknown horseshoe vortex strengths ($\Delta\Gamma_i$, $i = 1, N$), the normal force on each panel can be computed by adding the load carried by the bound and the two trailing vortices as shown in Reference 19. The load carried by any vortex segment is given by

$$\Delta\mathbf{F} = \rho\mathbf{V}_e \times \Delta\Gamma\boldsymbol{\delta}, \tag{3}$$

where $\mathbf{V}_e$ is the local velocity at the midpoint of the vortex segment and $|\boldsymbol{\delta}|$ is the length of the vortex segment. In the planar vortex lattice model, $\mathbf{V}_e$ is approximated as

$$\mathbf{V}_e = U_\infty\mathbf{i} - \beta U_\infty\mathbf{j} + U_\infty\alpha\mathbf{k} \tag{4}$$

and $\boldsymbol{\delta}$ is given by

$$\boldsymbol{\delta} = \delta x\,\mathbf{i} + \delta y\,\mathbf{j}. \tag{5}$$

The total normal force on each panel can be computed from equation (3) as

$$\Delta F_Z = \rho U_\infty \Delta\Gamma[(y_2 - y_1) + \beta(x_2 - x_1)] - \rho\beta U_\infty \Delta\Gamma(x_3 - x_1) + \rho\beta U_\infty \Delta\Gamma(x_4 - x_2), \quad (6)$$

where (x_1, y_1), (x_2, y_2), (x_3, y_3) and (x_4, y_4) are the four corner points of each panel (Figure 2).

The resulting lift coefficient can be calculated by numerical integration as

$$C_L = \frac{1}{\frac{1}{2}\rho U_\infty^2 S} \sum_{i=1}^{M \times N} \Delta F_Z, \quad (7)$$

where S is the wing area.

The pitching and rolling moment coefficients can be calculated similarly by numerical integration.[19]

2.2. *Separated flow model*

In this model a non-planar vortex lattice model is employed, i.e. the lattice divides the lifting surface into panels which are generally non-planar. The basic difference in vortex pattern between this model and the attached flow model is in the formation of free vortex sheets representing the wakes adjoining the sharp edges where separation occurs. To simulate separation along sharp edges, for each of the N leading edge panels, one of the trailing vortices (the left one for port panels and the right one for starboard panels) is suppressed; instead of taking it downwards to the trailing edge and then to infinity downstream, it is taken upwards until it meets the leading edge and is then continued into the fluid to form a free vortex line (Figure 3). Each of these vortex lines is composed of a series of straight line segments, except for the last segment which extends semi-infinitely downstream. The direction of any finite segment is unknown and is determined as a part of the solution, but the final semi-infinite segment is aligned with the free stream direction.

The problem considered here involves the strengths of the vortices ($\Delta\Gamma_i$) and the direction cosines of the free vortex segments as the basic unknowns. In the present numerical study these unknowns are obtained by simultaneously satisfying the requirements that

(a) the normal component of the velocity is zero at each control point and
(b) each vortex segment except the final semi-infinite one in each line of the wake is force-free.

Since the strengths and positions of the free vortices are both unknowns, an iterative procedure is set up for the solution. To start with, the initial direction of the free vortex segments is taken as the mean flow direction as argued by Kuchemann,[20] i.e. at an angle $\alpha/2$ to the main stream. With this prescribed wake shape, the unknown strengths $\Delta\Gamma_i$ are obtained by satisfying the flow tangency condition at all collocation points. The set of linear algebraic equations can be written as

$$[B_{ji}]\{\Delta\Gamma_i\} = \{W_j\}, \quad (8)$$

where

$$W_j = \begin{cases} -U_\infty \sin\alpha \cos\Gamma + U_\infty \cos\alpha \sin\beta \sin\Gamma & \text{for the port wing,} \\ -U_\infty \sin\alpha \cos\Gamma - U_\infty \cos\alpha \sin\beta \sin\Gamma & \text{for the starboard wing.} \end{cases} \quad (9)$$

The subsequent iterative procedure involves the following steps.

(i) With each vortex strength known ($\Delta\Gamma^{(n-1)}$, where n is the current iteration number), each finite wake segment is aligned with the computed velocity at its midpoint, starting at the separation points. In adjusting the downstream endpoint of each segment in this way, an

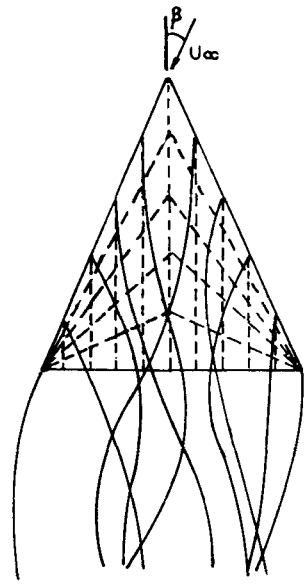

Schematic of leading edge separation vortices

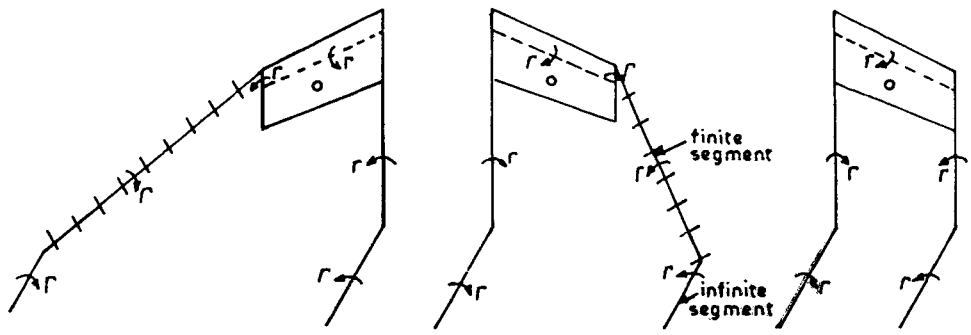

Vortex pattern on port leading edge panel

Vortex pattern on starboard leading edge panel

Vortex pattern on other panel

Figure 3. Separated flow model for wing in sideslip

inner iteration is necessary to repeat the process since the final positions of the segment midpoints do not coincide with the positions when the velocities were calculated at them. In the present algorithm, as argued by Maskew,[21] in computing the velocity at the midpoint of a finite segment, the influence of the entire vortex line on which that segment lies is ignored, rather than just that of the local segment.

(ii) With the wake fixed in the new position, the influence coefficient matrix B_{ji} is recalculated and new vortex strengths are redetermined from the flow tangency condition.

The iterative loop is repeated until convergence is achieved. Once the final vortex strengths are known, the loading on a single panel can be obtained from equation (3) as before. However, in the

non-planar vortex lattice mode, $\mathbf{V}_e$ and $\boldsymbol{\delta}$ are given by

$$\mathbf{V}_e = \mathbf{U}_\infty \cos\alpha \cos\beta \mathbf{i} - U_\infty \cos\alpha \sin\beta \mathbf{j} + U_\infty \sin\alpha \mathbf{k} + u\mathbf{i} + v\mathbf{j} + w\mathbf{k}, \tag{10}$$

$$\boldsymbol{\delta} = \delta x \mathbf{i} + \delta y \mathbf{j} + \delta z \mathbf{k}, \tag{11}$$

where u, v and w are the perturbation velocity components. The load carried by each 'bound' vortex segment in each panel can be obtained[22] from equation (3):

$$\Delta F_x = \rho U_\infty \Delta\Gamma[-U_\infty \cos\alpha \sin\beta + v)\delta z - (U_\infty \sin\alpha + w)\delta y], \tag{12}$$

$$\Delta F_y = \rho U_\infty \Delta\Gamma[(U_\infty \sin\alpha + w)\delta x - (U_\infty \cos\alpha \cos\beta + u)\delta z], \tag{13}$$

$$\Delta F_z = \rho U_\infty \Delta\Gamma[(U_\infty \cos\alpha \cos\beta + u)\delta y + (U_\infty \cos\alpha \sin\beta - v)\delta x]. \tag{14}$$

The above expressions can be used for calculating the load due to the trailing vortices on the wing. In spanwise panelling, the length of the trailing vortex in each panel is taken as extending from the quarter-chord point of the panel to the quarter-chord point of the adjacent panel in the same chordwise strip, and the perturbation velocity components (u, v, w) are calculated at the midpoint of this length. It can be noted here that for the trailing vortices, $\delta y = \delta z = 0$.

Once the total load on each panel has been computed, the resulting lift coefficient can be calculated by numerical integration as

$$C_L = \sum_{i=1}^{M \times N} (\Delta F_z \cos\alpha - \Delta F_x \sin\alpha \cos\beta + \Delta F_y \sin\alpha \sin\beta)/\tfrac{1}{2}\rho U_\infty^2 S. \tag{15}$$

The pitching and rolling moment coefficients can be computed by numerical integration.[22]

3. COMPUTATIONAL DETAILS

Two computer programs have been developed in FORTRAN IV for attached and separated flow models. To make the programs applicable for both zero and non-zero angle of sideslip, the complete wing surface is discretized and the condition of symmetry is not imposed. For the attached flow model, increasing the number of panels leads to increased accuracy and an optimum vortex lattice of 8 × 12 is used for the entire lifting surface. For the separated flow model, a restriction on the number of spanwise divisions is imposed by Almosnino[23] to prevent the generation of exaggerated induced velocities on the midpoint of a free vortex segment owing to the influence of the vortex segment next to it. In the present approach the same criterion is used and an optimum lattice of 8 × 8 is adopted in this case. With the lattice of 8 × 8 the convergence in the iterative loop is usually fast. The iteration is terminated when the change in normal force is below 2%. This accuracy is usually achieved within nine iterations for all configurations studied. Results are obtained on the Horizon III minicomputer.

4. RESULTS AND DISCUSSION

The results obtained by the present numerical models for both attached and separated flows are shown in Figures 4–6 for a delta wing of aspect ratio 1·0. In Figure 4 the normal force coefficient is shown as a function of the angle of attack. The results obtained for the symmetric case are compared with the Mook and Maddox solution[5] and the experimental data of Peckham.[24] To illustrate the effect of flow separation, the attached flow results are also plotted in the same figure. The predicted values of lift are identical up to about 5° incidence; beyond this the difference becomes significant, indicating the effect of leading edge separation.

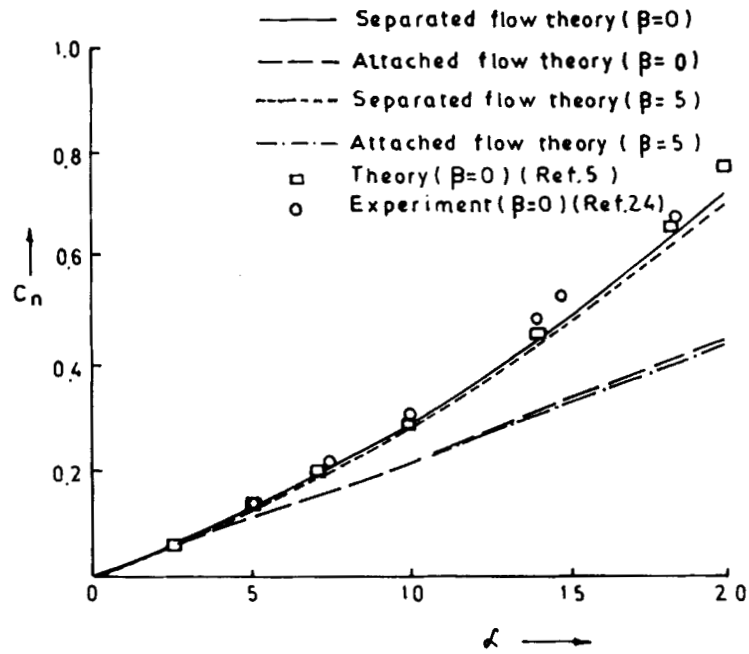

Figure 4. Variation of normal force with angle of attack

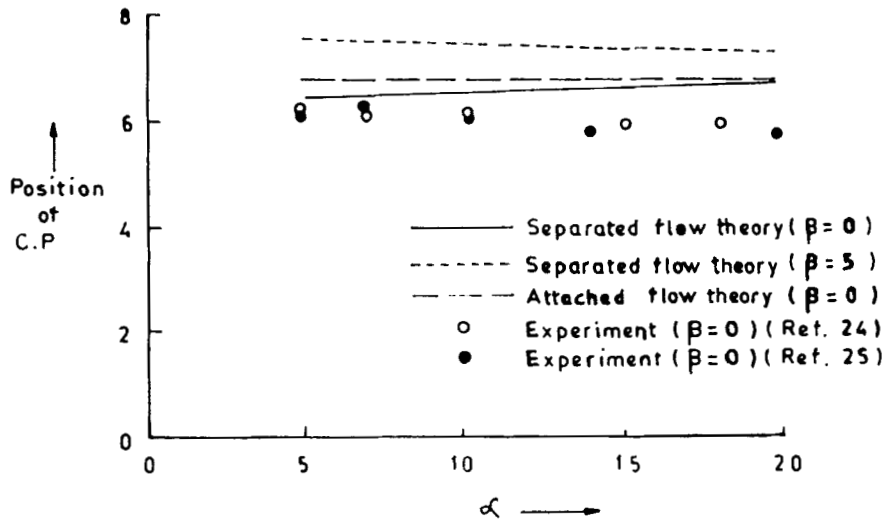

Figure 5. Variation of position of centre of pressure with angle of attack

The results obtained for the asymmetric case when the wing is in sideslip are also shown in Figure 4. These results indicate that the variation in normal force due to sideslip is negligible for both attached and separated flow cases.

The position of the centre of pressure is plotted as a function of the angle of attack in Figure 5. The comparison with experimental values[24, 25] is not satisfactory except at smaller angles of

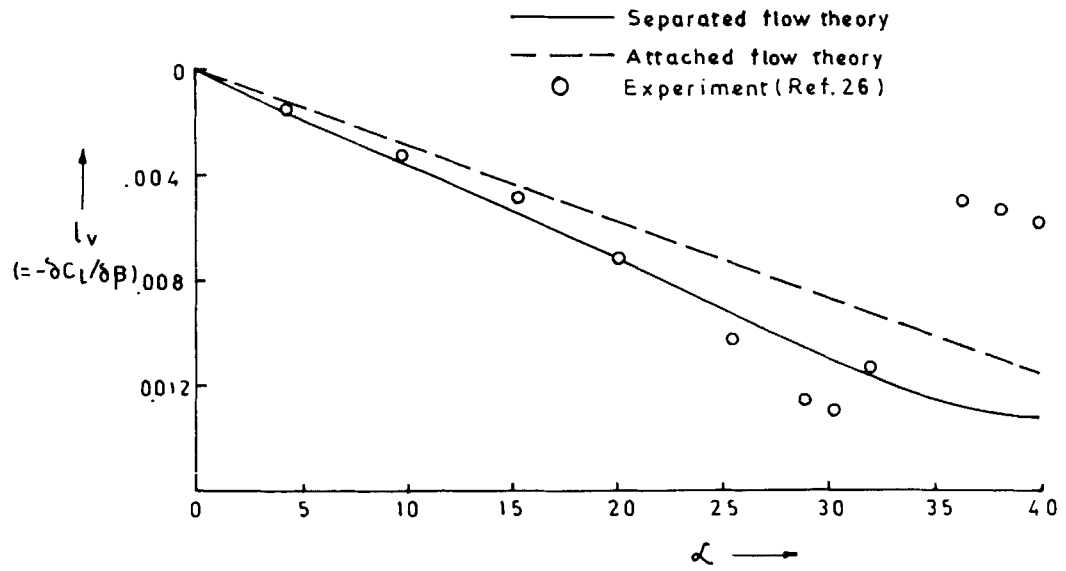

Figure 6. Variation of lateral stability derivative with angle of attack

attack. This is possibly due to the fact that the pitching moment characteristics are more sensitive to wing panelling than are the lift characteristics, and a better agreement may perhaps be obtained with proper panelling. However, the difference between the attached and separated flow solutions appears to be small.

The separated flow solution for the asymmetric case shows a significant change in position of the centre of pressure compared to the symmetric case. The centre of pressure appears to move towards the trailing edge with increasing sideslip angle.

The variation of the rolling moment l_v ($= \partial C_l/\partial\beta$, with β based on $\pm 5°$) with the angle of attack α is shown in Figure 6. The agreement of the separated flow solution with the experimental data[26] is reasonably good except at very high angle of attack. The discrepancy at high angle of attack is presumably due to bubble-type flow separation from the wing leading to stall, the effect of which is not taken into account in the theoretical model.

The solutions obtained by the attached flow theory, also shown in Figure 6, compare well with the experimental results up to about $\alpha = 20°$. The rolling moment is characterized by the difference in load on the two wings, and the simple attached flow theory can evidently calculate this difference in the two wings loads despite its inability to calculate individual wing loads accurately at moderate-to-high angle of attack.

The variation of rolling moment with sideslip angle β is presented in Figure 7 for a delta wing of aspect ratio 0·71, for which experimental values are available.[27] The solutions obtained by Jones' theory,[17] which depend on two parameters α/γ and β/γ (where γ is the wing half-apex angle), are also shown in the figure. The solutions obtained by the separated flow theory agree well with the experimental results. The discrepancy of the solution with Jones' theory is small and is perhaps attributable to the fact that Jones' theory[17] is based on the assumption of conical flow.

The rolling moment coefficients calculated by both the attached and separated flow theories are found to be approximately linear with the angle of sideslip. However, the discrepancy between the two solutions becomes significant at high values of β.

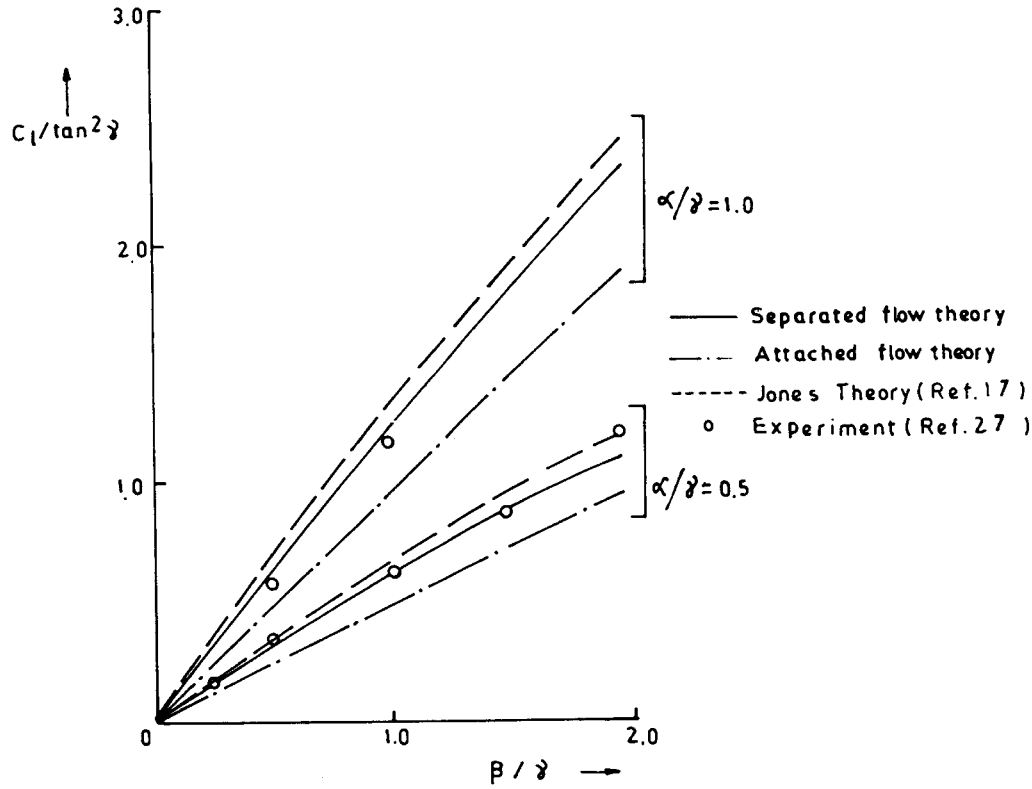

Figure 7. Effect of sideslip on rolling moment

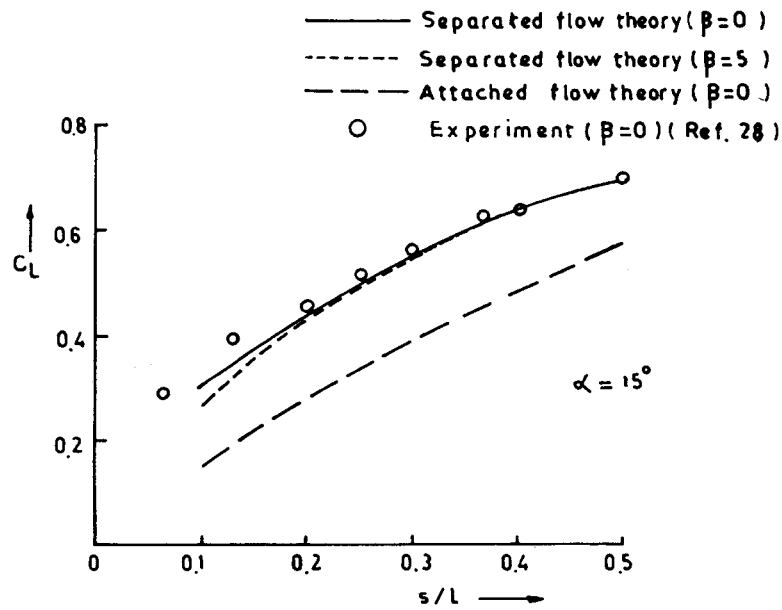

Figure 8. Effect of slenderness ratio on lift

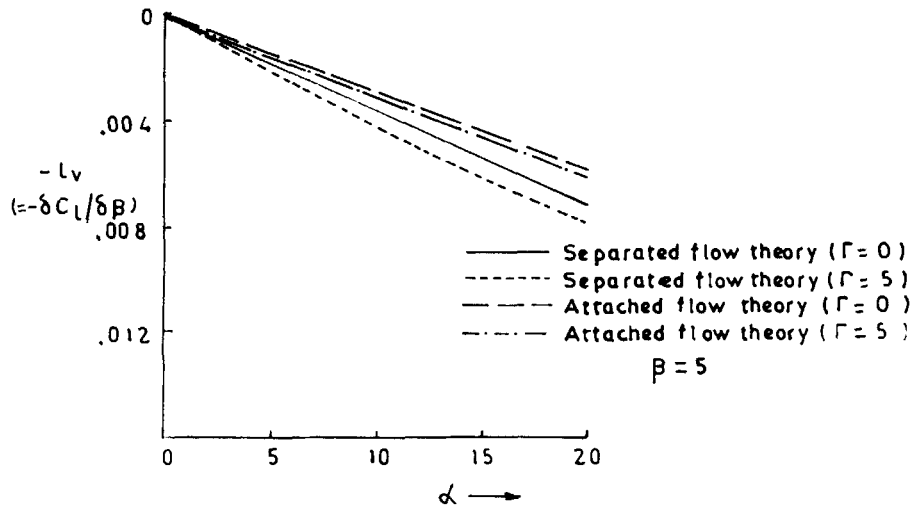

Figure 9. Effect of dihedral on lateral stability derivative

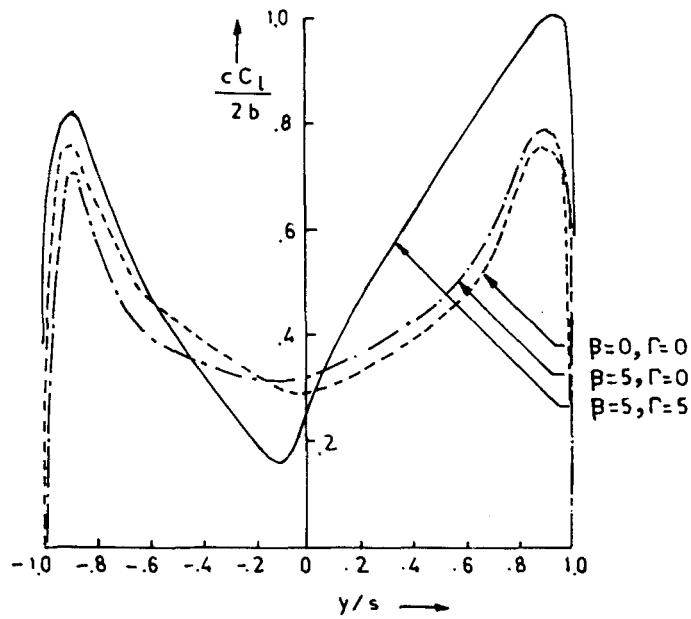

Figure 10. Spanwise load distribution

In order to check the applicability of the present method to other configurations, the calculated lift coefficients are compared with the experimental data of Kuchemann[28] for delta wings of varying aspect ratio. The comparison for the symmetric case appears to be good (Figure 8). The variation of lift due to sideslip again seems to be small except for very slender delta wings of slenderness ratio 0·1 (i.e. aspect ratio 0·4).

The effect of the wing dihedral on the rolling moment stability derivative is presented in Figure 9. Both attached and separated flow solutions show a significant increase in $-l_v$ with

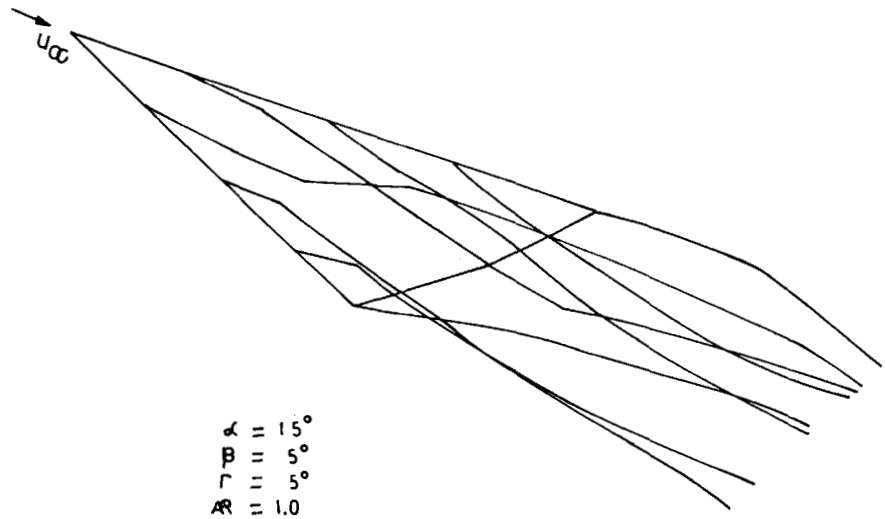

Figure 11. Roll-up of leading edge vortices on a delta wing (with sideslip)

increasing dihedral even though the variation of the normal force with the dihedral is found to be small.

An explanation of this feature follows from the spanwise load distributions ($c\bar{C}_l/2b$, with c the local chord, $\bar{C}_l$ the local lift coefficient and b the wing span) shown in Figure 10. It is seen that compared to the zero-dihedral wing, the loading on the starboard is increased while that on the port is decreased for a dihedral wing. This results in an increase of $-l_v$ for the dihedral wing even though the total normal force remains relatively unchanged.

The separation of vortices from the leadng edges of a dihedral wing and the subsequent roll-up is obtained by using an 8 × 8 lattice for the entire wing and is shown in Figure 11.

5. CONCLUDING REMARKS

Attached and separated flow models have been developed for calculation of the potential flow about delta wings at incidence and in sideslip. The separated flow model is capable of predicting accurately the aerodynamic forces and moments at high incidence until bubble-type separation occurs. Numerical solutions obtained by the two models indicate a significant change in lift, particularly at moderate-to-high angle of incidence, indicating the effect of separation from sharp leadng edges. However, the difference in pitching and rolling moments is not so pronounced, particularly for small sideslip angle.

Numerical examples indicate that the lift is virtually independent of the angle of sideslip whereas the rolling moment is found to vary linearly with the angle of sideslip. The effect of dihedral on the lift is seen to be marginal but is quite significant for the rolling moment.

REFERENCES

1. R. Legendre, 'Flow in the neighbourhood of the apex of a highly swept wing at moderate incidence', *ARC Report 16 796*, 1954.
2. C. E. Brown and W. H. Michael, 'On slender delta wings with leadng edge separation', *NACA TN 3430*, 1955.

3. K. W. Mangler and J. H. B. Smith, 'Calculation of the flow past slender delta wings with leading edge separation', *Report Aero 2593*, Royal Aircraft Establishment, Farnborough, 1957.
4. J. H. B. Smith, 'Improved calculations of leading edge separation from slender delta wings', *Report 66970*, Royal Aircraft Establishment, Farnborough, 1966.
5. D. T. Mook and S. A. Maddox, 'Extension of a vortex lattice method to include the effects of leading edge separation', *J. Aircraft*, **11**, 127–128 (1974).
6. C. Rehback, 'Numerical investigation of vortex systems issuing from separation line near the leading edge', *NASA TT F-15*, 530, 1974.
7. O. A. Kandil, D. T. Mook and A. H. Nayfeh, 'Nonlinear prediction of aerodynamic loads on lifting surfaces', *J. Aircraft*, **13**, 22–28 (1976).
8. F. T. Johnson, P. Lu, G. W. Brune, J. A. Weber and P. E. Rubbert, 'An improved method for the prediction of completely three-dimensional aerodynamic load distributions on configurationswith leading-edge separation', *AIAA Paper 76 417*, 1976.
9. F. T. Johnson, P. Lu, E. N. Tinoco and M. A. Epton, 'An improved panel method for the solution of three-dimensional leadng-edge vortex flows: Vol. I—Theory document', *NASA CR-3278*, 1980.
10. A. J. Peace, 'A multi-vortex model of leading edge vortex flows', *Int. j. numer. methods fluids*, **3**, 543–565 (1983).
11. E. C. Polhamus, 'A concept of vortex lift of sharp-edge delta wings based on a leading edge-suction analogy', *NASA TN D-3767*, 1966.
12. S. A. Jepps, 'A method for computing attached and separated flow past slender bodies', *BAC (MAD) Report MSN 218*, 1976.
13. S. A. Jepps, 'The computation of vortex flows by panel methods', *Von-Karman Institute Lecture Series 5*, 1978.
14. C. Rehbach,'Calcul numérique d'ecoulements tridimensionnels instationnaries avec nappes tourbillonnaires', *Rech. Aerospatiale*, **5**, 289–298 (1977).
15. J. H. B. Smith, 'Inviscid fluid models, based on rolled-up vortex sheets for three-dimensional separation at high Reynolds number', *Paper No. 9, AGARD Lecture Series No. 94*, 1978.
16. D. I. Pullin, 'Calculations of the steady conical flow past a yawed slender delta wing with leading edge separation', *Imperial College Aero Report 72 47*, 1972.
17. I. P. Jones, 'Flow separation from yawed delta wings', *Comput. Fluids*, **3**, 155–177 (1975).
18. J. Katz, 'Lateral aerodynamics of delta wings with leading edge separation', *AIAA J.*, **22**, 323–328 (1984).
19. M. A. Javed and G. J. Hancock, 'Application of vortex lattice methods to calculate L_v (rolling moment due to sideslip)', *Report No. EP-1038, Queen Mary College, London*, 1980.
20. D. Kuchemann, 'A nonlinear lifting-surface theory for wing of small aspect ratio with edge separations', *Report Aero 2540*, Royal Aircraft Establishment, Farnborough, 1955.
21. B. Maskew, 'Numerical lifting surface methods for calculating the potential flow about wings and wing-bodies of arbitrary geometry', *Ph.D. Thesis*, Loughborough University, 1972.
22. P. E. Rubbert,'Theoretical characteristics of arbitrary wings by a nonplanar vortex lattice method', *Report D6-9244*, The Boeing Co., 1964.
23. D. Almosnino, 'High angle-of-attack calculation of the subsonic vortex flow on slender bodies', *AIAA J.*, **23**, 1150–1156 (1985).
24. D. H. Peckham, 'Low speed wind-tunnel tests on a series of uncambered slender pointed wings with sharp edges', *Report Aero 2613*, Royal Aircraft Establishment, Farnborough, 1958.
25. G. E. Bartlett and R. J. Vidal, 'Experimental investigation of influence of edge shape on the aerodynamic characteristics of low aspect ratio wings at low speeds', *J. Aero. Sci.*, **22**, 517–533 (1955).
26. D. Levin and J. Katz, 'Dynamic load measurement of delta wings undergoing self-induced roll oscillations', *AIAA Paper 82-1320*, 1982.
27. J. K. Harvey, 'Some measurements on yawed slender delta wings with leading edge separation', *ARC R and M 3160*, 1961.
28. D. Kuchemann, *The Aerodynamic Design of Aircraft*, Pergamon Press, 1978, p. 378.